Sextos, A., Manolis, G., Athanasiou, A., & Ioannidis, N. (2017). Seismically induced uplift effects on nuclear power plants. Part I: Containment building rocking spectra. *Nuclear Engineering and Design*, *318*, 276-287. https://doi.org/10.1016/j.nucengdes.2016.12.035

SEISMICALLY INDUCED UPLIFT EFFECTS ON NUCLEAR POWER PLANTS. PART 1: CONTAINMENT BUILDING ROCKING SPECTRA

A. G. Sextos[1, 2], G. D. Manolis[1*], A. Athanasiou [1], N. Ioannidis[1]

[1]Department of Civil Engineering, Aristotle University of Thessaloniki, Greece
[2]Department of Civil Engineering, University of Bristol, UK
* Corresponding Author

ABSTRACT

Current nuclear regulatory codes specify design considerations for extreme seismic scenarios, focusing primarily on the response of the containment structure of a nuclear power plant. However, in current state-of-practice and in most seismic regulations worldwide, the consideration of soil-structure interaction and potential development of geometrically nonlinear effects, such as rocking and sliding with uplift, is not taken into consideration. To explore this issue, a refined 3D finite element model of a typical nuclear power plant containment structure is developed, comprising solid elements for the soil and foundation, plus shell elements for the structure. The aim is identification of foundation-soil separation phenomena under a suite of ground motions with distinct frequency content. At first, harmonic excitations are used, for both cases of stiff sand and rock subsoil profiles, leading to rocking spectra that depict the displacement demand in connection with nonlinear separation. Clear influence zones can be distinguished, especially in the low frequency bands for the stiff sand case. Next, three subsets of 30 ground motion records are carefully selected and grouped in ensembles according to their frequency content, normalized to a PGA of 0.36g, which corresponds to the highest design acceleration in Europe. Ground motions with low mean frequency content are observed to lead to the onset of geometrically nonlinear phenomena, along with a higher displacement demand. The interplay between ground motion characteristics, dynamic properties of the containment structure and stiffness of the soil is also highlighted. More specifically, it is shown that stiff containment structures on soft soils are more prone to foundation uplift. This possibility is often neglected in design codes and the consequence is that under certain circumstances, damage may be caused to the internal power generation equipment..

Keywords: nuclear power plants; containment structure; mechanical equipment; soil-structure-foundation interaction

INTRODUCTION

Power generation from nuclear energy is a dependable source, but it is also associated with high environmental, financial and social risks, as the recent Fukushima, Japan nuclear power plant accident of March 11, 2011 from the tsunami triggered by the M_w=9.0 Tohoku earthquake vividly demonstrated. This event resulted in a new round of research on nuclear energy, not only with regards to its production, but also on the design specifications for nuclear reactor structures. Focus is primarily on one of the most important edifices of a nuclear power plant (NPP), namely the nuclear containment building, as this structure protects critical equipment used for nuclear energy generation. Design of NPP has long been performed on the basis of standard guidance (American Society of Civil Engineers (ASCE), 2005, 1998; European Commission, 1996) that prescribe design considerations for seismic intensity measures of appropriately low mean annual frequency of exceedance, focusing primarily on the response of containment structures. Until recently, however, research conducted on the interaction between the containment building and the underlying soil has been scarce, even though the problem was very early identified (Newmark and Hall, 1969). Moreover, issues of geometrical nonlinearities at the building-soil interface, such as uplift and sliding, have also been neglected due to the complexity of numerical modeling and particularly due to the fact that most widely used codes available for soil-structure-interaction (SSI) analysis (Lysmer et al., 1999) were traditionally addressing the problem in the frequency domain.

On the other hand, recent research has identified cases of NPP and high-hazard nuclear waste facilities where nonlinear interface issues need to be carefully accounted during seismic design and assessment. Saxena and Paul (Saxena and Paul, 2012) studied the effect of slip and separation due to soil-foundation-structure interaction (SFSI) on the seismic response of the foundation of a nuclear reactor containment building, using 3D finite element method (FEM) analysis. They also showed that any increase of the foundation's embedment depth reduces the horizontal slip and vertical separation phenomena from the underlying soil. Next, Bhaumik and Raychowdhury (Bhaumik and Raychowdhury, 2013) studied the seismic response of an internal shear wall of a reactor using a 2D FEM model considering nonlinear soil-structure interaction. They concluded that containment buildings on soft soils have higher plasticity demands as compared to those founded on competent rock, and are prone to manifestation of geometrically nonlinear effects. Jeremic et al. (Jeremić et al., 2013) showed that the frequency content of the ground excitation greatly influences the response of both surface and embedded containment building foundations, especially when nonlinear effects are present. Recent studies (Kumar et al., 2015) concluded that

nonlinear effects, in the presence of SFSI, may alter the dynamic characteristics of the structure itself, something which primarily depends on the frequency content of the seismic excitation. Other studies have further demonstrated a thorough non-linear SSI methodology for NPP constructions in the time domain, incorporating the presence of material (Kabanda et al., 2015) and geometrically nonlinearities (Coleman et al., 2015; Huang et al., 2010) at the soil-foundation interface, such as gapping and sliding. All these studies highlight the potentially significant impact of nonlinear phenomena, particularly for ground intensities exceeding the Design Basis Earthquake. Notably, the original design value in Fukushima was 0.26g (updated to 0.45g in 2009), while the recorded one was 0.56g. Similar exceedances have also been reported (Coleman et al., 2015) elsewhere in Japan (e.g., Kashiwazaki-Karina, 0.20g versus 0.32g recorded) and the United States (at the 1,865-MW North Anna Power Station in Mineral, Va, 0.18g versus 0.26g recorded in 2011 during a magnitude 5.8 event). In fact, the latter event was the only time an earthquake has forced a U.S. nuclear plant offline and also the first U.S. plant to experience an event that exceeded its design acceleration (within a time window of three seconds).

As the social impact of a possible NPP failure is tremendous as it the case of leakage of radioactive materials, more recent regulations explicitly address the issue of nonlinear SSI by distinguishing nonlinearities in the site response, large-strain soil material behavior, geometric phenomena at the foundation-soil interface, and nonlinear behavior (i.e., cracking) of structures and mechanical equipment. These documents, like the Idaho National Laboratory (INL) methodology (Spears and Coleman, 2014) and the forthcoming Appendix B of the new version of the ASCE 4 Standard (American Society of Civil Engineers (ASCE), 2015) take a significant step further by introducing new concepts, approaches and tools. However, the nature of these provisions is still non-mandatory.

Given the above emerging need for refined analytical and numerical studies, the objective of this work is to shed some further light on nonlinear seismic soil-structure interaction of NPPs by:

(a) correlating the frequency content of the excitation with geometrically nonlinear interface phenomena (i.e., uplift and sliding) of the containment building, in the form of "rocking spectra" (Makris and Konstantinidis, 2002) for different soil profiles. We note that the geometrically nonlinear soil-structure interaction has been studied in the past, see for instance (Kennedy et al., 1976; Nakamura et al., 2010, 2007). The concept of rocking spectra is used herein and has been extrapolated from other systems exposed to seismic risk such as base-isolated generic structures (Politopoulos, 2010), bridges (Anastasopoulos et al., 2013), masonry walls (Costa et al., 2013) or even laboratory and hospital equipment

(Cosenza et al., 2014; Konstantinidis and Makris, 2009), free-standing blocks (Dimitrakopoulos and DeJong, 2012; Voyagaki et al., 2013) and monuments (Makris and Vassiliou, 2013).

(b) identify the frequency range of the seismic excitation, as a function of soft and firm foundation soils, that will provoke nonlinear effects at the soil-foundation interface of a NPP.

(c) use the complex nonlinear response of the soil-containment building system as input for the assessment of the internal equipment seismic demand (presented in Part II of this work).

In sum, the FEM modeling and analysis of this two-stage, complex structural assessment is accomplished using the ABAQUS (2010) software (Dassault Systèmes, 2014). The case studied, the assumptions, the methodological steps and the observations made are presented in the following.

OVERVIEW OF THE NPP STUDIED

A typical Westinghouse Pressurized Water Reactor (PWR) containment structure is studied in this work, comprising a circular base slab, an upright cylinder as the main structure and a hemispherical dome, as shown in Fig. 1. The PWR has a height of 85.8m, wall thickness of 1.5m and is partially embedded in the supporting ground. The reinforcement of the containment is composed of Ø40 mm bars at 80mm spacing, running both ways at the inner and outer faces of the cylindrical R/C wall, continuing within the spherical dome with an assumed effective concrete cover of 100mm (Hu and Lin, 2006). Material properties are summarized in (Hu and Liang, 2000) as well as in Table 1 and they are defined within the elastic region on the basis of the envisaged linear elastic response performance objective of the containment building.

In order to numerically simulate the seismic behavior of this containment-foundation structural system, a nonlinear dynamic analysis is carried out using the Newmark-beta method. Two soil conditions are considered, namely stiff sand and competent rock, as being representative of the ground conditions in the Central and Eastern United States, respectively, see (Bolisetti et al., 2014).

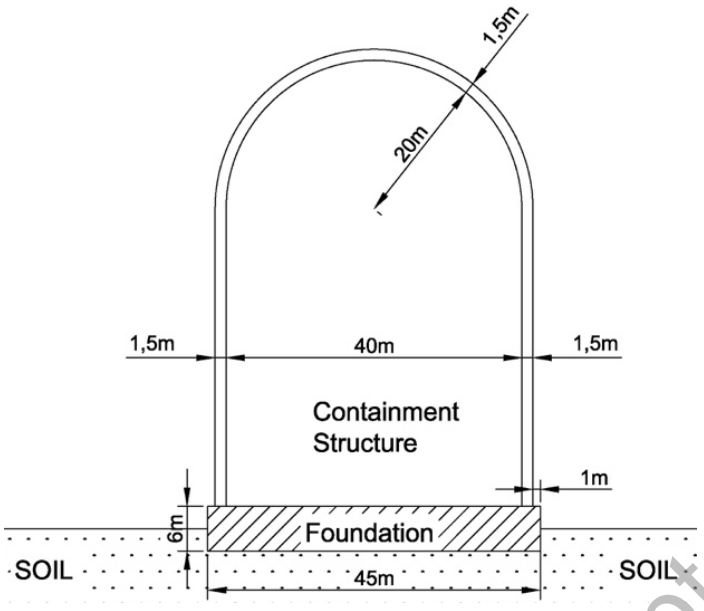

Fig. 1: Geometry of the containment building studied.

Table 2: Material characteristics of the containment building studied.

Concrete	
Compressive Strength f_c (MPa)	35
Tensile Strength f_t (MPa)	2
Modulus of Elasticity E_c (GPa)	28
Poisson's Ratio	0.2
Strain at compressive strength ε_{cu}	0.0035
Density ϱ (kg/m^3)	2500
Steel	
Modulus of Elasticity E_s (GPa)	200
Yield Stress f_y (MPa)	460
Density ϱ (kg/m^3)	7850

Both soil sites consist of a 100m deep, uniform (i.e., single layer) profile and rest on elastic, viscously damped bedrock. The shear wave velocity of the two studied soil profiles are taken equal to V_s=300m/s (with unit weight of γ=20.1 kN/m^3) and V_s=2500m/s (and unit weight of γ=23.3 kN/m^3), for the sand and rock case, respectively. Particularly for the first case, an equivalently reduced, linear shear modulus is assumed for the purposes of site response analysis equal to $G= 0.7G_0$ (i.e., 70% of its initial value) as an approximate means of considering soil nonlinearity under strong ground motion. In general, NPP structures are commonly constructed on firm soils and rock, but there are cases where the NPP is founded on soft soil (Ding and Xia, 2014). Then, measures are taken such as soil pre-loading, deep embedment, seismic isolation and piles to ameliorate the problem.

The internal configuration of a typical PWR is composed of an R/C wall structure, whose purpose is to support the mechanical components which are vital for the normal operation of the NPP. These components are primarily the nuclear reactor and the main cooling system, which comprises the steam generators and the circulation pumps, along with the piping system that interconnects them. The structural integrity of the cooling system is of paramount importance and must be maintained under all conditions. Thus, depending on the level of a possible cracking, problems in the circulation and the heat dissipation ability of the system may occur, particular under a loss-of-coolant accident *(*LOCA*)* event (Muzumdar and Meneley, 2009).

In order to assure the structural integrity of the cooling system, the main strategy proposed by the Boiler and Pressure Vessel Code (BPVC), see ASME 2010a (American Society of Mechanical Engineers (ASME), 2010a) is to keep the nominal stress that develop in the system components under the allowable stress, which in turn depends on the material itself and the operating temperature as discussed in ASME 2010b (American Society of Mechanical Engineers (ASME), 2010b). The BPVC divides nominal stress into a primary and a secondary component, representing stresses from equilibrium forces and from displacement compatibility, respectively. The BPVC allows exceedance of the nominal stress for temporary actions such as earthquake, depending on the characterization of the piping. For instance, nuclear Class 1 piping nominal stress (S_n) must not exceed three times the allowable stress intensity (S_m):

$$S_n < 3S_m \tag{1}$$

In this joint paper, the seismically-induced state of stress in the main cooling system piping network is evaluated by taking into account external SSI phenomena manifested in the NPP containment building, and more precisely on the geometrically nonlinear phenomena such as uplift, sliding and rocking across the soil-foundation interface (discussed in more detail in Part II). To this purpose, a detailed 3D FEM model of the internal structure is created, whereby both the internal R/C walls and the nuclear reactor with its main cooling system are modeled. Four different analysis approaches are comparatively examined, as discussed in the section below.

FINITE ELEMENT MODELLING OF THE SOIL-NPP SYSTEM

The FEM model comprises solid elements for the foundation and soil and shell elements for the structure (upright cylinder and dome). More specifically, (a) the soil is discretized using the ABAQUS 3D stress element C3D8R (8-node linear brick, reduced integration, hourglass control), (b) the foundation by the 3D stress element C3D20R (20-node quadratic brick, reduced

integration) and (c) the upper circular cylindrical structure plus its roof by the shell element S8R (8-node doubly curved thick shell, reduced integration).

Next, the surrounding soil domain is circular cylindrical so as to match the geometry of the superstructure, which is axisymmetric. The domain radius is 135m, which is three times the diameter of the foundation to avoid wave reflection associated with the external boundaries. The FEM mesh becomes progressively denser in the near field. The maximum size of the individual finite elements (L_m) was chosen so as to balance computational effort and accuracy (i.e., by respecting $L_m < V_s/(a\, f_n)$, where V_s the shear wave velocity of the soil, f_n Nyquist frequency and a the corresponding factor varying from 5-10). Since our focus is on the quantitative description of geometrically nonlinear phenomena, a coarser mesh was developed and tested against the original refined mesh. Minimal differences were observed insofar as the manifestation of separation at the soil-foundation interface was concerned. Finally, the natural frequency of the soil mass was confirmed also by hand calculations, once the size of elements was finalized. The final FEM model is depicted in Fig. 2.

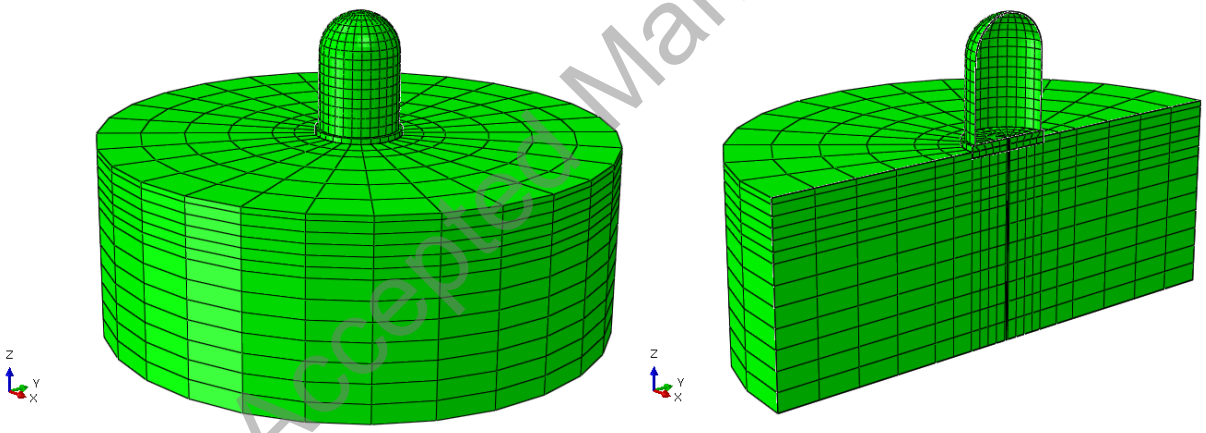

Fig. 3: 3D meshed model of the entire NPP soil-foundation-structure problem

Next, three groups of boundary conditions were defined for (a) the base and (b) the sides of the soil mass, as well as (c) for the soil-foundation interface. The soil mass base has all degrees-of-freedom (DOF) fixed, except for the translational DOF in X-axis, which serves as input for the seismically-induced accelerations. For the lateral boundary conditions, 14 "PIN" constraints are used for all outer circumferential nodes at each elevation "Level" of the soil mass. These 14 vertical "Levels" are defined in reference to the FEM mesh along the Z-axis (Fig. 3). The aforementioned "Levels" reproduce the shear behavior between neighboring soil elevation layers and also prevent

the lateral spread of the soil mass from gravitational loads. An additional set of lateral springs and dashpots (Lysmer et al., 1969) was also used at the boundaries of the soil domain.

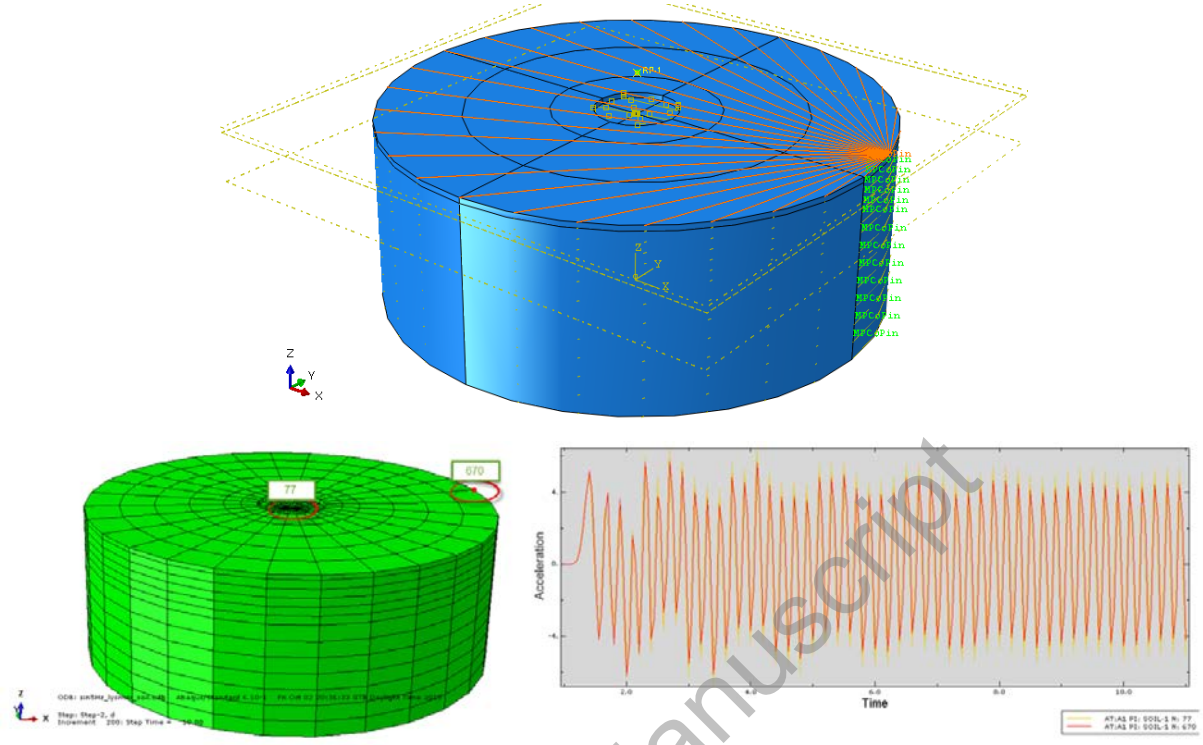

Fig. 4: Lateral Boundary Conditions – MPC constraints (top) and verification of non-reflective boundary performance of the FE mesh (bottom).

Interaction properties are defined for the soil-foundation interface. More specifically, for the connection of the lateral sides and the base of the embedded foundation with the soil, "TIE" constraint is used for the modal analysis and the ensuing linear time-stepping analysis, while "Surface-to-Surface contact" constraint is used for the nonlinear analyses. In addition, for the nonlinear case a unique interaction property is used, which comprises the "Penalty Contact" for the tangential direction with $\mu_{\sigma\tau}$=0.7 as the static coefficient of friction (Srinivasan et al., 1985), and the "Hard Contact" for the normal direction. The dynamic coefficient of friction is ignored, since we wish to determine the onset of nonlinear sliding and not to trace its entire path with time.

In order to include the entire NPP mass, a concentrated (lumped) mass encompassing the mass of the mechanical equipment and of the support walls inside the containment building is placed with the aid of the "Inertia" command from the "Engineering features" list at a reference point, i.e., the center of mass. Then, this reference point's DOF are connected to the surface of the outer structure's base, using the "Coupling" constraint and specifically the "Continuum Distributing" coupling type.

Finally, an equivalent 5% damping was prescribed to the FE model based on the G-γ-D curves of the soil profile for the level of soil shear strain γ that resulted from site response analyses with a ground acceleration whose response spectrum matched the design one (CEN, 2004a). Then, the appropriate Rayleigh parameters were defined so as to fix 5% damping at two discrete frequencies, i.e., the eigen frequencies of the fixed containment structure (3.78Hz) and that of the SSI system (0.743Hz for soft soil and 6.22Hz for rock). The resulting alpha and beta Rayleigh parameters for soft soil and rock were a=0.39, b=0.035 and a=3.37 and b=0.00041, respectively.

NUMERICAL ANALYSIS OF THE SOIL-CONTAINMENT BUILDING SYSTEM

Six different cases were considered for the soil-structure system illustrated in Fig. 2, as listed below:

- *Case A1*: Standard *Modal Analysis* for the identification of modal frequencies, mode shapes and participation factors
- *Case A2*: *Response Spectrum Analysis* (RSA) of the containment building assumed to be fully fixed (RSA, no SSI). Use is made of the Eurocode 8 design response spectrum (CEN and European Committee for Standardization (CEN), 2004) for soil type A (rock) and C (moderate stiffness), ground acceleration a_g=0.36g and behaviour factor q=1.0 as the Design Basis Earthquake (DBE). It is noted that normally the design base earthquake is defined on the 10^{-4}/annum non-exceedance level, taken on the mean hazard curve. Since the present study does not refer to any specific site, the above EC8-compatible assumption is made. The aim is to assess the seismic demand that would be computed under conventional design approach.
- *Case A3*: *Linear Response History Analysis* (LRHA) of the NPP containment structure assuming rock supporting conditions (LRHA, no SSI). Thirty, three-component, hazard-compatible ground motions are selected and used as input directly at the base of the building, hence, both kinematic and inertial SSI phenomena are neglected. The scope is to assess the variation of response quantities in time ignoring SSI effects.
- *Case A4*: *Equivalent-linear Response History Analysis* of the NPP containment structure assuming soft soil supporting conditions (eLRHA, plus SSI). Soil compliance and the subsequent effect on the dynamic characteristics of the soil-structure system is addressed by modelling the near field soil domain with 3D finite elements. The modification of the bedrock motion due to the response of the overlying soil layer is inherent in the 3D site response analysis. Material nonlinearity of soils, as already mentioned, is considered with equivalent reduced shear modulus of $G=0.7G_0$. No uplift or sliding is taken into

consideration across the soil-foundation interface. This case represents the most advanced modelling of the soil-structure domain that is currently encountered in practice.

- *Case A5*: *Geometrically nonlinear, material equivalent-linear, Harmonic Analysis* of the NPP containment structure assuming soft soil supporting conditions and geometrically nonlinear SSI effects. In this case, uplift, sliding and rocking are explicitly modelled along the soil-foundation interface (NLRHA, plus SSI). Appropriate harmonic pulses were applied at the bedrock level instead of recorded ground motions. The aim is to plot response quantities and forms of nonlinear behaviour (sliding, uplift, coupled sliding/uplift) as a function of excitation frequency.
- *Case A6*: *Geometrically nonlinear, material equivalent-linear, Response History Analysis* Similar to A5, with a suite of 30, appropriately selected, recorded motions at the bedrock level. It is considered that this is the most comprehensive approach to date and is used to identify the potential implications of nonlinear SSI in a probabilistic manner. The response of the containment building is also used as the input motion for the building-only analysis of Case B2, in order to assess the seismic demand increase on the internal mechanical equipment (Part II).

It is noted that in cases A3-A5, the same thirty ground motions are used at the bedrock of the FEM model, to account for identical hazard conditions. Cases A2-A4 were studied mainly for verification purposes and are not further discussed herein.

Modal Analysis and Verification Tests (Case A1)

For the modal analysis of the NPP soil-foundation-structure system, only the translation modes of vibration of the structure are presented, to show the effect of soil versus rock sub-base on the natural frequencies of the soil-NPP system. More specifically, Figs. 4-5 depict the predominant mode of vibration of the structure on soft and rock soil, respectively. For the NPP on soft soil, the first mode of vibration corresponds to the natural frequency of the soil mass, which is calculated as 0.743Hz. This value closely resembles the hand-calculated value of 0.75Hz for the natural frequency of the soil mass viewed as a 1D soil column, using the simplified expression $f=V_s/4H$. Next, the 3rd eigenmode of vibration is the dominant translational mode of vibration for the structure alone, calculated as equal to 1.238Hz. For the rock sub-base, the natural frequency of the rock mass is 6.25Hz as calculated by hand and 6.223Hz from the FEM model, while the natural frequency of the structure alone is increased to 3.81Hz. The latter correlates well with the value of a similar NPP described in the literature (Zhao and Chen, 2013). By comparing these results, a remarkable increase can be seen in the predominant natural period of the NPP structure,

moving from rock (i.e., an equivalent fixed-base structure) to softer soil deposits. This leads to the conclusion that the SFSI phenomenon strongly influences the dynamic characteristics of the NPP containment structure.

Following modal analysis, verification tests were carried in the linear elastic range to establish the reliability of the FEM model and the effect of boundary truncation. For this verification process, 10 time-history analyses were conducted by using Ricker wavelets at the base of each soil/rock model, in the frequency range of 1.0-10.0 Hz with a 1Hz step. The key parameter was the relative displacement between the top of the containment structure and the foundation base. More specifically, the ratio of the maximum relative displacement for the NPP structure on soil to rock was calculated, for each frequency step in the records. It was clearly observed that this ratio is maximum at 1.0 Hz, a value close to the natural frequency of the soil mass (0.75Hz), and minimum at 6.0 Hz, a value close to the natural frequency of the rock mass (6.25Hz).

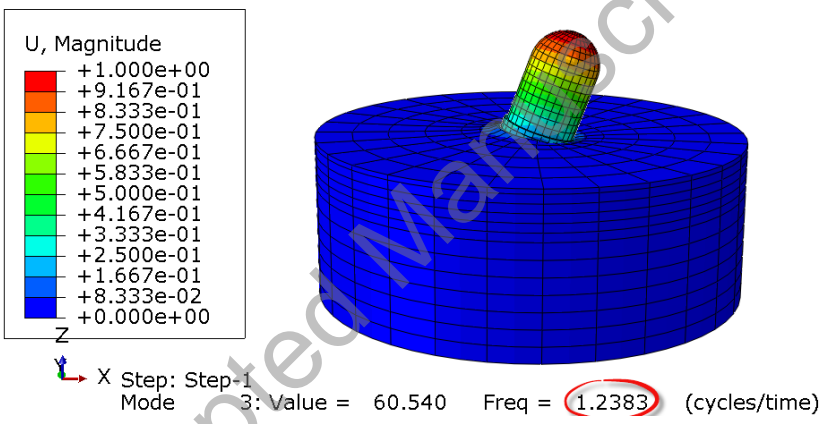

Fig. 5: Dominant X-translational mode of vibration for the NPP structure on soft soil

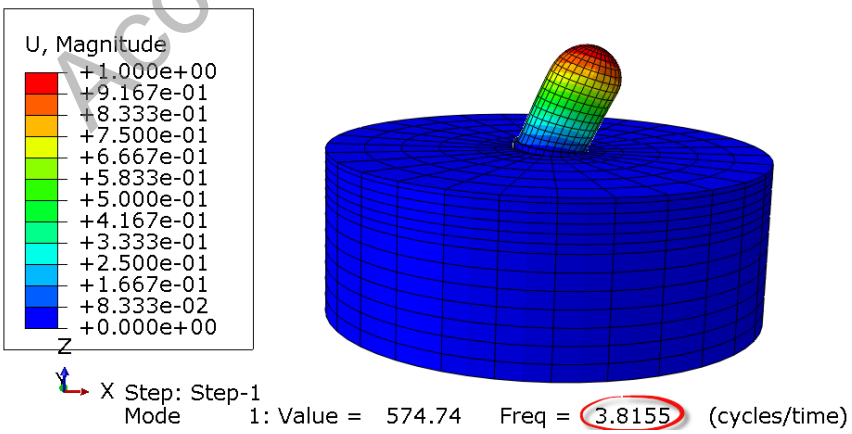

Fig. 5: Dominant X-translational mode of vibration for the NPP structure on rock

In addition, the verification test to account for boundary effects was conducted using a sine wavelet with a frequency content of 5.0 Hz, at the base of the model and in the absence of the containment

structure. In this way, a comparison of the translational acceleration responses at two key nodes was possible: One node was set at the center of the soil surface and another on the lateral soil boundary. The acceleration responses showed no distortion on the harmonic sine wavelets, indicating that no appreciable wave reflections take place within the FEM mesh.

Geometrically Nonlinear Analysis using Sinusoidal Pulses (Case A5)

Analysis outline

After verification of the NPP containment structure FEM model through modal and linear elastic analyses, a series of geometrically nonlinear analyses were conducted. These lead to the creation of rocking spectra, for an input comprising base excitations. Notably, the analysis was performed in the time domain using sinusoidal pulses after removing the transient stage. The excitation frequency ranged between 0.5 and 8.0 Hz, in increments of 0.5Hz, while the ground intensity varied from 0.2g to 1.0g, in 0.2g increments. In total, 16x5=80 nonlinear analyses were conducted for each type sub-grade (soil and rock), summing up to 160 analyses. To account for geometrically nonlinear phenomena, three key parameters were traced versus time: (a) Horizontal relative displacement between the central node of the bottom surface of the foundation and the corresponding central node at the soil interface, (b) vertical relative displacement of the aforementioned nodes and the (c) foundation tilt angle associated with uplift. The onset of sliding and rocking was assumed at the threshold values of 0.02m horizontal translation and 0.03m vertical uplift, respectively. These numbers correspond to 0.5 ‰ of the structure's horizontal and vertical dimensions, respectively. In addition, the horizontal displacement of the top of the containment structure was also measured.

Rocking Spectra

In Table 2, the rocking spectra for soft soil and hard rock are displayed, where we observe the geometrically nonlinear effect of separation in bands of frequencies and acceleration intensities for harmonic ground excitations. Next, Fig. 6-7 depict 4D plots for rocking spectra, with the 3rd (i.e., vertical) dimension corresponding to the maximum relative displacement computed of the top of the containment building with respect to its base and to the 4th (colored) dimension depicting the type of the geometrical nonlinearity. These rocking spectra for soft soil clearly illustrate the formation of "affection zones" that trigger the nonlinear separation between foundation and soil, primarily at low frequencies. More specifically, the frequency band of 0.5 - 1.0 Hz brackets the soil profile's natural frequency of 0.75Hz and this is where sliding and rocking is triggered. Furthermore, large displacements at the top of the structure are observed. A harmonic excitation of 1.0g intensity on the bedrock to soil interface may significantly amplify accelerations at the

surface of the soil during resonance. Of course, an actual earthquake strong ground motion is typically rich in a wider range of frequencies and is certainly not monochromatic, with the exception of near field pulses that may be dominated by a single pulse. Thus, the assumption of harmonic excitation is therefore clearly a more detrimental.

Nevertheless, even if it is considered as an upper bound in absolute terms, the effect of soil compliance on the type of geometrical SSI nonlinearity at the interface is evident: the NPP building studied, when founded on hard rock and excited with pulses of moderate to low frequency content (0.5<f<2.5Hz) may rock but it never slides (independently of the amplitude of excitation), whereas the same building on soft soil may easily slide even for bedrock amplitude 0.2g, while it can respond in a coupled sliding/rocking mode for stronger intensities. It is noted that pure rocking of the building on hard rock is also associate with its foundation embedment, which prevents sliding due to the non-deformability of the rock, thus promoting uplift.

Table 2: Rocking spectra qualitative display for a NPP containment building with partially embedded foundation on soft soil (top) and hard rock (bottom).

1.0	SR	SR	SR	SR	S											
0.8	SR	SR	SR	SR												
0.6	SR	SR	S	S												
0.4	SR	SR														
0.2		S														
α(g)/f(Hz)	0.5	1	1.5	2	2.5	3	3.5	4	4.5	5	5.5	6	6.5	7	7.5	8

1.0	R	R	R	R	R											
0.8	R	R	R	R												
0.6																
0.4																
0.2																
α(g)/f(Hz)	0.5	1	1.5	2	2.5	3	3.5	4	4.5	5	5.5	6	6.5	7	7.5	8

	No sliding / Rocking
	Sliding (S)
	Rocking (R)
	Sliding and Rocking (SR)

Overall, the containment building response under nonlinear SSI phenomena justifies the commonly held perception that massive, compact structures show rocking and/or overturning

tendencies at low frequencies and especially those close to their own rocking frequency. To give an absolute number, the highest uplift of the building's edge from the ground was 0.25m in the vertical direction, corresponding to an uplift angle of 0.32°. Again this corresponds to the most unfavorable case of purely sinusoidal excitation.

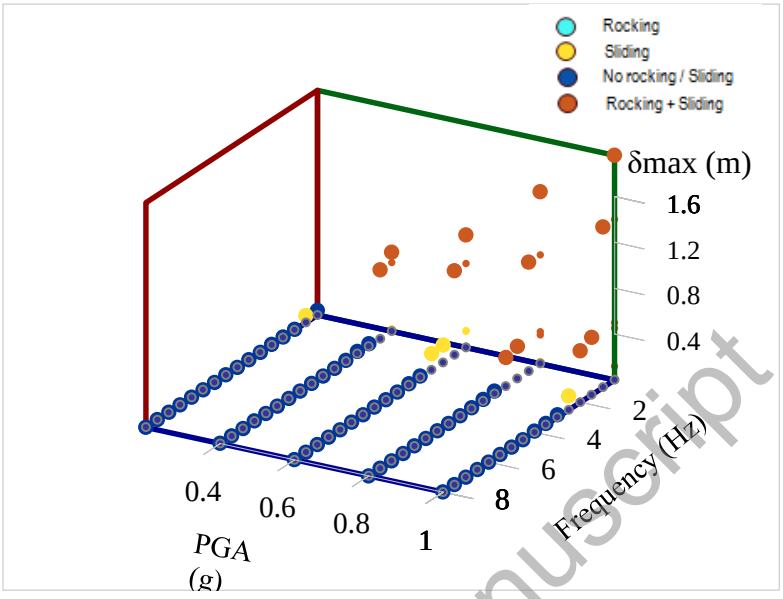

Fig. 6: 4D rocking spectra for the NPP containment building with half-embedded foundation on soft soil: Frequency and bedrock amplitude in the horizontal plane, relative displacement between top and base of the containment building in the vertical direction and colored illustration of the geometrical nonlinearity mode at the interface.

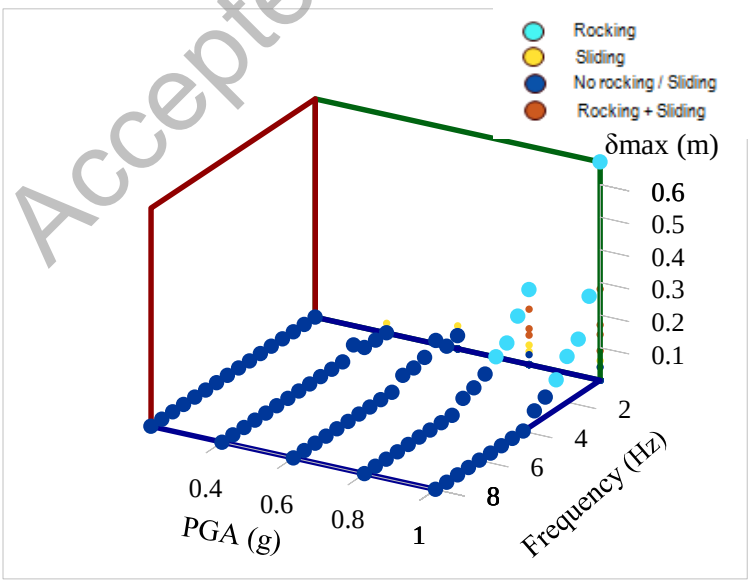

Fig. 7: 4D rocking spectra for a NPP containment building with half-embedded foundation on rock: Frequency and bedrock amplitude in the horizontal plane, relative displacement between top and base of the containment building in the vertical direction and colored illustration of the geometrical nonlinearity mode at the interface.

Table 3: Distribution of selected earthquake ground motions in terms of their mean period Tm

Subset Number	T_m Interval (s)	Number of Records
1	0.10 - 0.50	10
2	0.50 - 0.90	10
3	0.90 - 1.55	10

Table 4: Earthquake events and related information retrieved from the PEER-NGA database

ID	Earthquake (year)	Magn. M_w	Distance (km)	Site Class	Record Name	Subset
1	Parkfield (1966)	6.19	34.01	D	PARK_C08320.AT2	1
2	San Fernando (1971)	6.61	25.36	C	SFERN_ORR291.AT2	1
3	San Fernando (1971)	6.61	26.10	C	SFERN_L01021.AT1	2
4	Managua, (1972)	6.24	5.68	D	MANAGUA_A-MAN090.AT1	1
5	Friuli (1976)	6.5	20.23	C	FRIULI_A-TMZ000.AT1	1
6	Tabas (1978)	7.35	20.63	C	TABAS_DAY-TR.AT2	1
7	Coyote Lake (1979)	5.74	10.94	D	COYOTELK_G02050.AT1	1
8	Imperial Valley (1979)	6.53	17.65	D	IMPVALL_H-CX0225.AT1	2
9	Imperial Valley (1979)	6.53	12.99	D	IMPVALL_I-ELC180.AT1	2
10	Imperial Valley (1979)	6.53	43.15	D	IMPVALL_H-BRA225.AT1	3
11	Imperial Valley (1979)	6.53	29.07	D	IMPVALL_H-ECC092.AT2	3
12	Imperial Valley (1979)	6.53	19.44	D	IMPVALL_H-EMO000.AT1	3
13	Coalinga (1983)	6.36	39.97	C	COALLINGA_H-Z15000.AT1	3
14	Coalinga (1983)	6.36	52.86	D	COALINGA_H-COW000.AT1	3
15	White Narrows (1987)	5.99	20.68	D	WHITTIER_A-OR2010.AT1	3
16	Loma Prieta (1989)	6.93	30.89	D	LOAMP_CLD195.AT1	1
17	Loma Prieta (1989)	6.93	28.11	D	LOMAP_GOF160.AT1	2
18	Loma Prieta (1989)	6.93	63.49	E	LOMAP_A02043.AT1	3
19	Northridge (1994)	6.69	13.39	D	NORTHR_MUL009.AT1	2
20	Northridge (1994)	6.69	21.55	D	NORTHR_WPI316.AT2	3
21	Kobe (1995)	6.9	24.2	D	KOBE_KAK000.AT1	1
22	Kobe (1995)	6.9	43.58	D	KOBE_FK000.AT1	3
23	Kobe (1995)	6.9	46.73	D	KOBE_ABN000.AT1	2
24	Kocaeli (1999)	7.51	99.69	D	KOCAELI_AT090.AT2	2
25	Kocaeli (1999)	7.51	95.02	D	KOCAELI_BUR090.AT2	3
26	Chi-Chi (1999)	7.62	4.96	C	CHICHI_TCU78-E.AT1	1
27	Chi-Chi (1999)	7.62	69.11	C	CHICHI_HWA033-N.AT2	2
28	Chi-Chi (1999)	7.62	43.31	C	CHICHI_TCU048-N.AT2	2
29	Chi-Chi (1999)	7.62	39.7	C	CHICHI_CHY029-N.AT2	3
30	Taiwan Smart1 (1986)	6.32	68.38	D	SMART1_40I01EW.AT1	3
	Site Classes according to NEHRP classification: Site Class A ($V_{s,30}$≥1500m/s), Site Class B (760m/s<$V_{s,30}$≤1500m/s, Site Class C (360m/s<$V_{s,30}$≤760m/s, Site Class D (180m/s<$V_{s,30}$≤360m/s, Site Class E ($V_{s,30}$≤180m/s).					

Nonlinear Response History Analysis (Case A6)

For the nonlinear analyses using strong ground motions, three subsets of 10 ground motion records each, for a total of 30, were selected in appropriate ensembles with a distinct mean frequency content, from a pool of 300 properly categorized ground motions (Katsanos et al., 2014). This decision was deliberately made in order to cover, in an unbiased way, a wide range of frequencies required for the generation of rocking spectra. Clearly, in case of a specific design or assessment study, a comprehensive probabilistic seismic hazard would be required and the ground motions would have been selected accordingly. To quantify the dominant frequency content of the records used, the mean period T_m was used (Kottke and Rathje, 2008) as a means to retain the ensemble as uniformly distributed as possible. The value of T_m indicates whether the frequency content of the record is categorized as high, moderate or low. The parameter T_m derives from the following equation:

$$T_m = \frac{\sum C_i^2 * \frac{1}{f_i}}{\sum C_i^2}, for\ 0.25Hz \le f_i \le 20Hz \text{ with } \Delta f \le 0.05\ Hz \quad (2)$$

In the above, *Ci* are the Fourier amplitude coefficients of the Fourier Amplitude Spectrum (FAS), *fi* are the discrete Fast Fourier Transformation (FFT) frequencies between 0.25 and 20.0 Hz and Δf is the frequency interval used in the FFT.

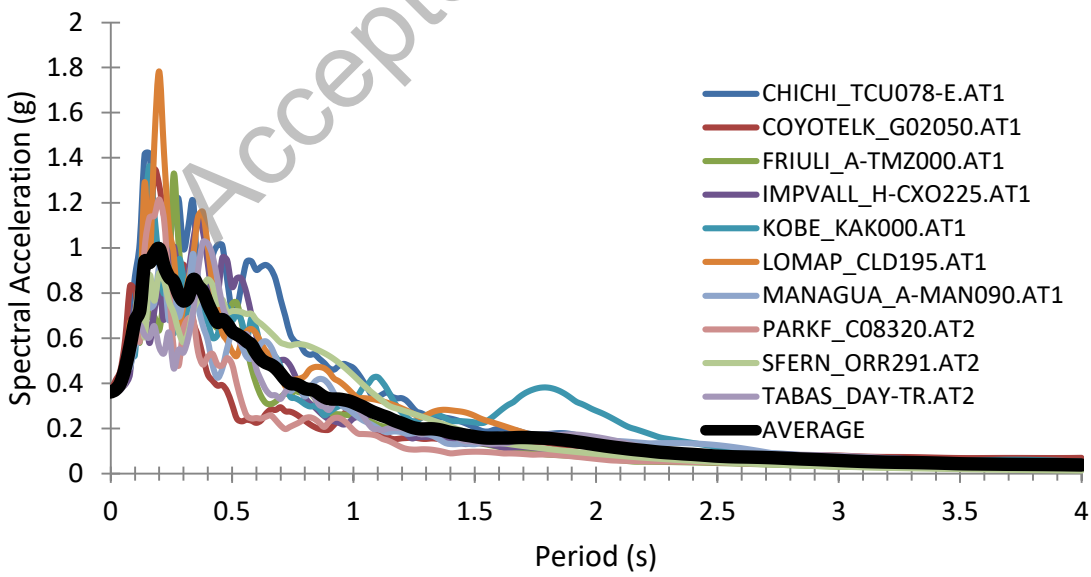

Fig. 8: Acceleration response spectra for the first subset of ground motions with low mean period content ($0.1<T_m<0.5$sec).

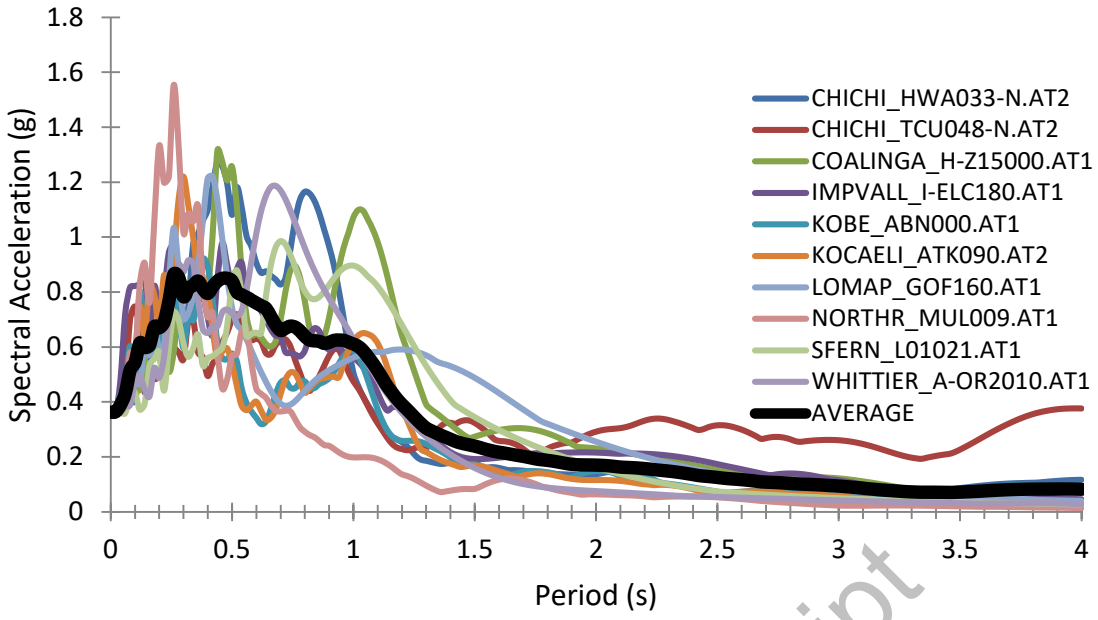

Fig. 9: Acceleration response spectra for the second subset of ground motions with mean period content ($0.5<T_m<0.9$sec).

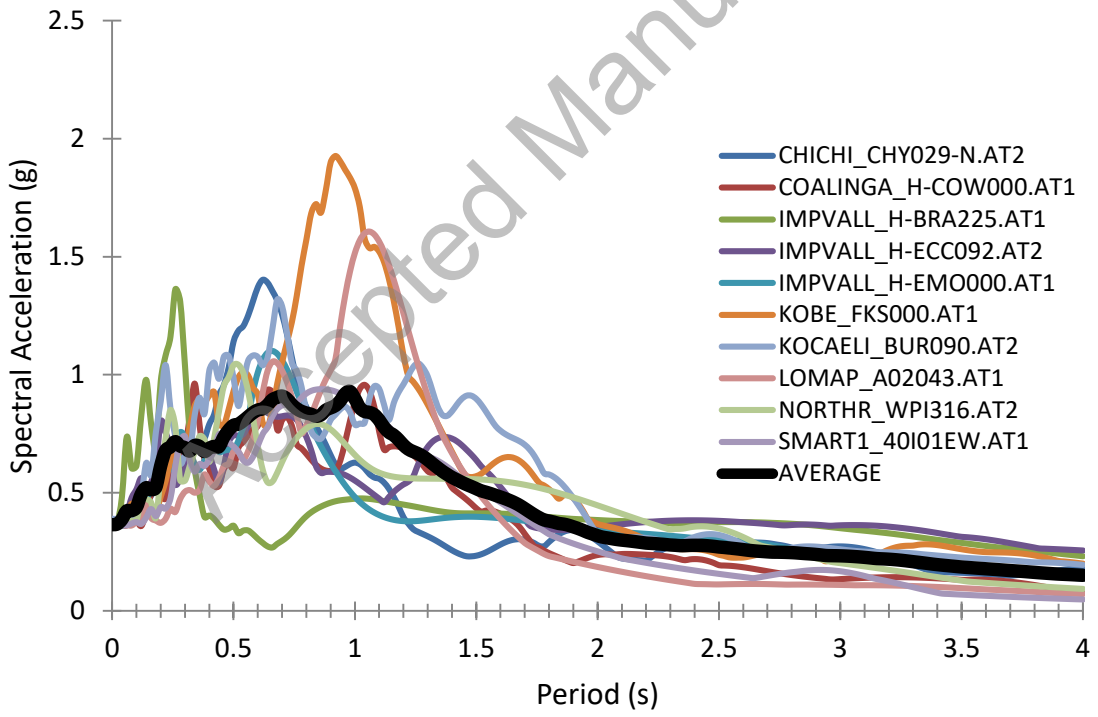

Fig. 10: Acceleration response spectra for third subset of ground motions with mean period content ($0.9<T_m<1.55$sec)

Based on the above criteria, the metadata of the three subsets of records and the summary of the ground motions used are given in Tables 3 and 4, respectively. All 30 records were normalized to a PGA of 0.36g, which is the highest PGA of the design earthquake possible in Europe (CEN,

2004b, 2004c), chosen to ensure that development of geometrically nonlinear phenomena at the foundation-soil interface. It is noted that, this level of intensity refers to the bedrock level according to EC8, hence, further amplification is expected during site response analysis, particularly for soft soil. This level of Intensity Measure may be higher or lower than a Design Basis Earthquake (DBE) in other sites, for a critical limit state for seismic design of safety-related Structures, Systems and Components (SSCs), as proposed by the nuclear regulatory codes (ASCE, 1998 and ASCE, 2005). Figures 8-10 illustrate the individual acceleration response spectra of the aforementioned subsets, along with the mean spectrum for each subset. The mean period values T_{m1}, T_{m2} and T_{m3} are 0.21, 0.52 and 0.98 sec for the three subsets, respectively. The measured parameters and thresholds, for which sliding and rocking are possible, are the same as for the sinusoidal excitations case. All (geometrically) nonlinear SSI analyses with equivalent linear material properties were conducted for both the soft soil and rock conditions, however, results are only plotted for the first case.

Table 5 summarizes the response of the NPP containment structure founded on soil in terms of maximum rocking and/or sliding values. Next, Figs. 11-13 display the maximum relative displacement (top to base) of the containment structure, for the three ground motion record suites, with color as an indicator of the type of geometrically nonlinear effect observed. Finally, Fig. 14 depicts the calculated probability of each type of nonlinear effect at the soil-foundation interface (i.e., sliding, rocking and coupled sliding/rocking), for the three distinct mean period ground motion subsets.

Table 5: Maximum rocking and/or sliding values for the NPP containment structure on soft soils: Three ground motion sets

T_{m1} (0.1 - 0.5 sec)			**T_{m2} (0.5 - 0.9 sec)**			**T_{m3} (0.9 - 1.55 sec)**		
ID	Sliding (m)	Rocking (m)	ID	Sliding (m)	Rocking (m)	ID	Sliding (m)	Rocking (m)
#01	-	-	#03	0.035	0.06	#10	0.008	
#02	0.008	-	#09	0.006	-	#11	0.06	0.16
#04	-	-	#13	0.025	0.02	#12	0.015	0.01
#05	-	-	#15	0.018	0.01	#14	0.04	0.08
#06	-	-	#17	0.03	0.09	#18	0.08	0.1
#07	-	-	#19	-	-	#20	0.04	0.06
#10	0.006	-	#23	-	-	#22	0.1	0.16
#16	-	-	#24	-	-	#25	0.025	0.08
#21	-	-	#27	-	-	#29	0.03	0.07
#26	-	-	#28	-	-	#30	0.06	0.12

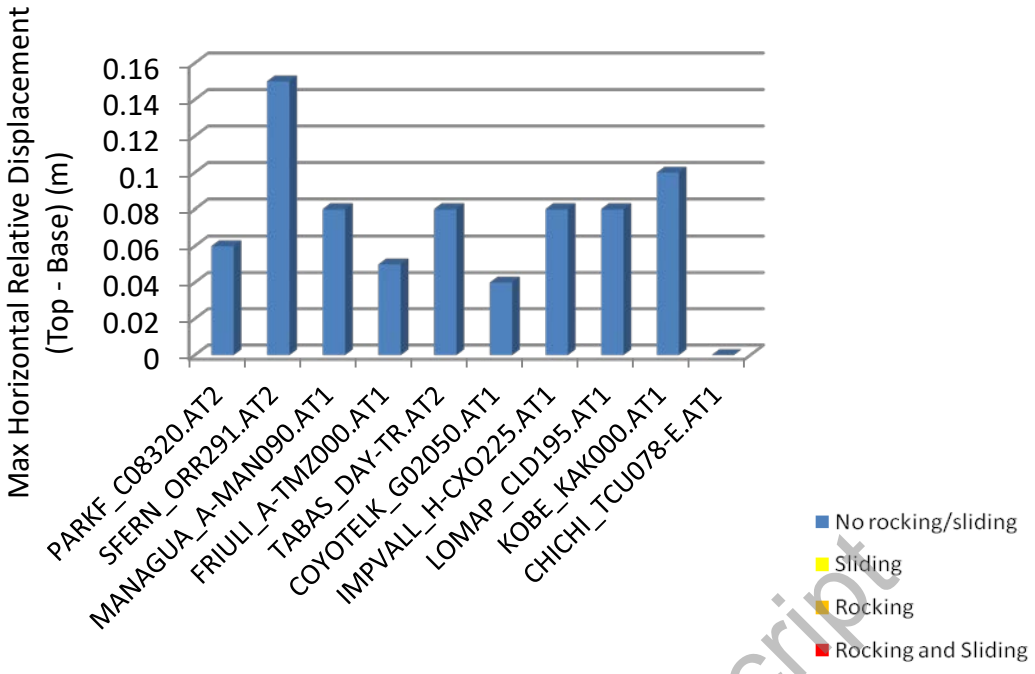

Fig. 6: Maximum horizontal relative displacement (top to base) of the NPP containment structure on soft soils, for the first subset of ground motions as a function of the geometrically nonlinear effect that appears

($0.1<T_m<0.5$sec).

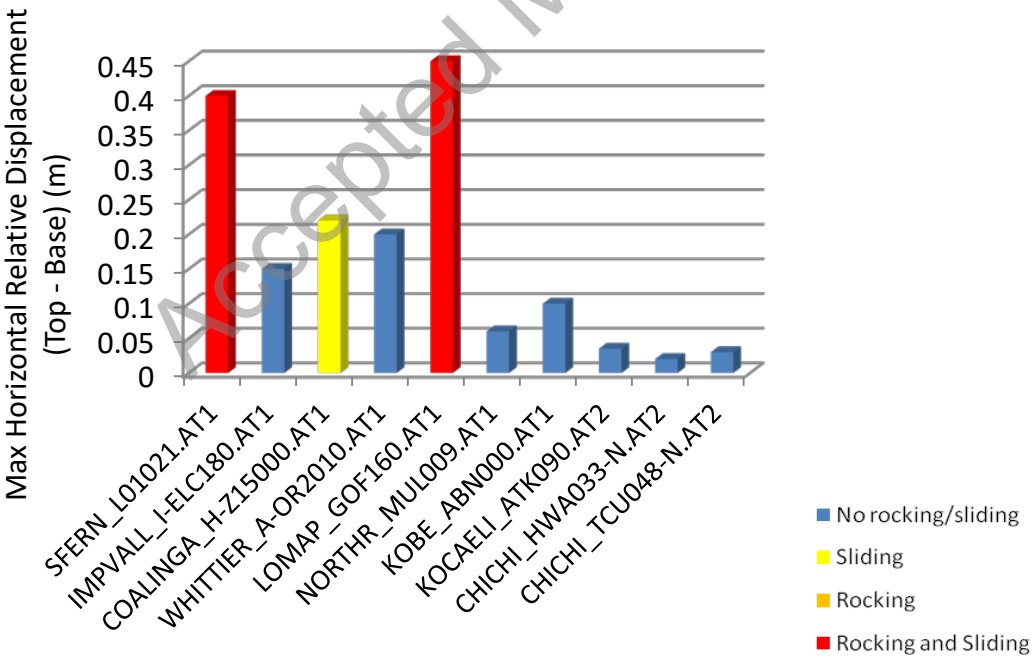

Fig. 7: Maximum horizontal relative displacement (top to base) of the NPP containment structure on soft soils, for the first subset of ground motions as a function of the geometrically nonlinear effect that appears

($0.5<T_m<0.9$sec).

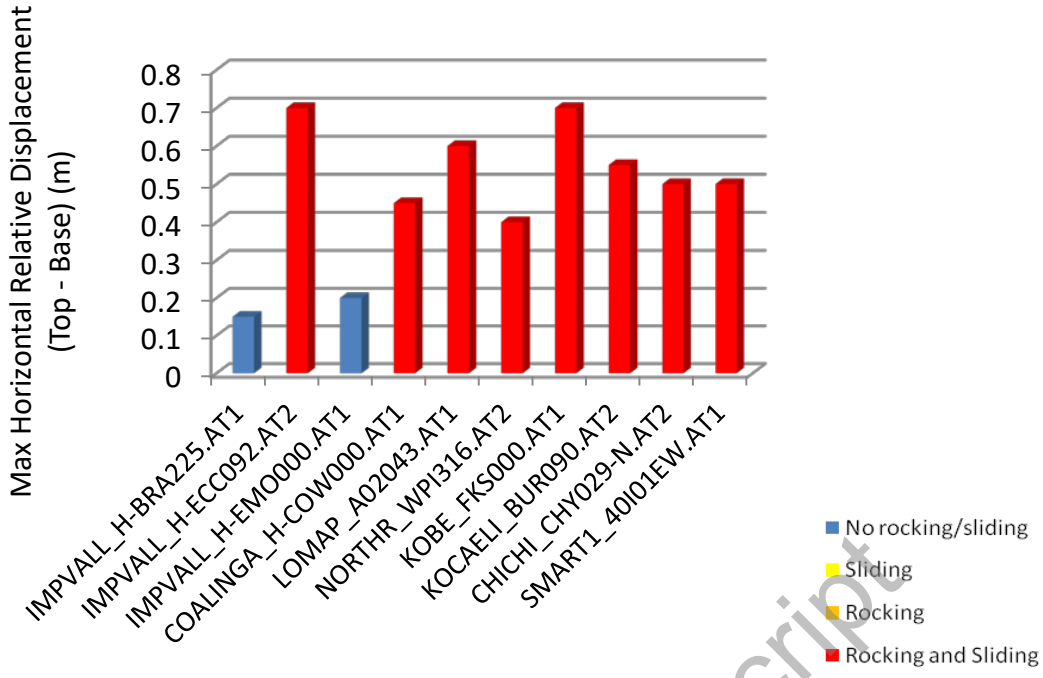

Fig. 8 Maximum horizontal relative displacement (top to base) of the NPP containment structure on soft soils, for the first subset of ground motions as a function of the geometrically nonlinear effect that appears

($0.9<T_m<1.55$sec).

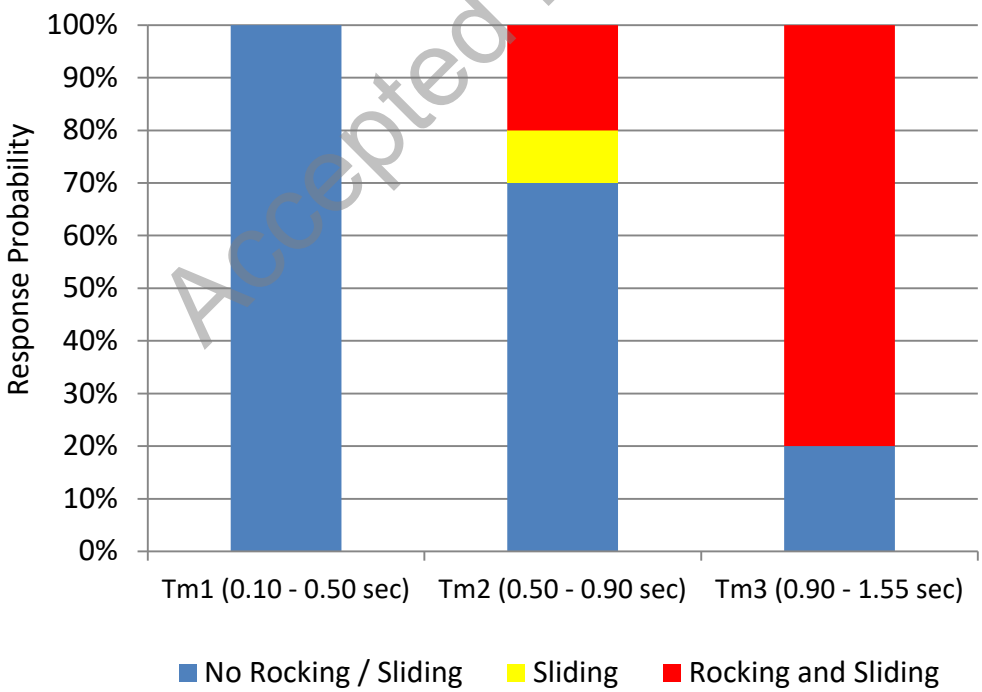

Fig. 9: Probability of appearance of geometrically nonlinear effects for the NPP containment structure as a function of the three ground motion subsets

From all the above figures, it is evident that ground motions with a low mean frequency content lead to the onset of geometrically nonlinear phenomena, along with a higher displacement demand. The interplay between the ground motion characteristics for the NPP containment structure founded on soil is also clearly highlighted. Also, nonlinear response is not observed at high frequency bands. This response is in line with the rocking spectra presented for the case of sinusoidal excitation and the soft soil conditions (Fig. 6), and confirms that moderate (0.5<Tm<0.9sec).and particularly long period pulses (0.9<Tm<1.55sec) may induce significant and coupled nonlinear phenomena such as sliding and rocking at the foundation-soil interface of the building. It can be further observed that ground motions that trigger uplift are followed by huge displacement demands, because of the height of the NPP containment structure, while ground motions that do not trigger any nonlinear effect produce minor deformations in the structure that do not exceed 0.16m. In absolute terms, this may be of the order of 0.7m relative horizontal displacement between the building top and base (equal to approximately 1% drift) for a peak ground acceleration of 0.36g. It is noted that, statistically speaking, the vertical component in case of long period motions must have been influenced, at least to some extent, by the vertical component even though the latter is not on average as pronounced as for near-field excitations. However, this is a subject that warrens further study.

Given the stiffness of the containment building, this sliding/rocking behavior may not necessarily lead to structural damage or extensive cracking but can be associated with abruptly increased seismic demand to the internal mechanical equipment, as discussed in Part II. Finally, for the rock foundation substratum, there is no triggering of geometrically nonlinear effects and the minimal displacement demands observed, which do not exceed 0.03m.

CONCLUSIONS

For NPP containment structures, which house all the power generating equipment and are considered as the most critical component of the entire plant, current regulatory codes provide design specifications based on Basis Design or Beyond Design Basis Earthquakes (BDBE). Nevertheless, soil-structure interaction and particularly nonlinear phenomena associated with sliding and rocking of the containment building under BDBE events are not addressed by modern seismic codes and regulatory documents, with the exception of the (non-mandatory) new version of ASCE 4 standards. The present study presents a detailed FE modeling of the holistic soil-structure system excited and then studies its response under both harmonic pulses and actual (yet unbiased) sets of recorded ground motions. The analyses clearly demonstrate that in the presence of soft soil formations, nonlinear soil-foundation-structure interaction and associated geometric

effects, such as rocking and sliding, are possible. These phenomena are observed for moderate to low frequency ground motions (0.5-1.0 Hz) even at relatively low, i.e., comparable to the design ground shaking intensities (0.2-0.4g). Notably, the same frequency/intensity bands are identified from the analyses in the time domain using harmonic or recorded bedrock accelerations. The above combination of frequency content and amplitude may lead to significant relative displacements in the containment building. Even if the latter is treated as a rigid body on the basis of its high stiffness, the potential effect of this complex dynamic behavior on the seismic demand of the internal mechanical equipment is yet to be examined. This phenomenon is addressed in Part II of this work.

REFERENCES

American Society of Civil Engineers (ASCE), 2015. Seismic Analysis of Safety-Related Nuclear Structures and Commentary, ASCE 4-15 (forthcoming). Reston, Virginia, Virginia.

American Society of Civil Engineers (ASCE), 2005. Seismic design criteria for structures, systems and components for nuclear facilities, in: ASCE 43-05. Reston, Virginia.

American Society of Civil Engineers (ASCE), 1998. Seismic design criteria for structures, systems and components for nuclear facilities, ASCE 4-98. Reston, Virginia, Reston, Virginia.

American Society of Mechanical Engineers (ASME), 2010a. Boiler and Pressure Vessel Code Section III.

American Society of Mechanical Engineers (ASME), 2010b. Section II, Part D: Properties (metric). ASME Boil. Press. Vessel Code.

Anastasopoulos, I., Loli, M., Georgarakos, T., Drosos, V., 2013. Shaking Table Testing of Rocking—Isolated Bridge Pier on Sand. J. Earthq. Eng. 17, 1–32. doi:10.1080/13632469.2012.705225

ASCE, 1998. American Society of Civil Engineers (ASCE) Seismic Analysis of Safety-Related Nuclear Structures and Commentary. In: ASCE 43-05, Reston, Virginia.

Bhaumik, L., Raychowdhury, P., 2013. Seismic response analysis of a nuclear reactor structure considering nonlinear soil-structure interaction. Nucl. Eng. Des. 265, 1078–1090. doi:10.1016/j.nucengdes.2013.09.037

Bolisetti, C., Whittaker, A.S., Mason, H.B., Almufti, I., Willford, M., 2014. Equivalent linear and nonlinear site response analysis for design and risk assessment of safety-related nuclear structures. Nucl. Eng. Des. 275, 107–121. doi:10.1016/j.nucengdes.2014.04.033

CEN, 2004a. European Standard EN 1998-1. Eurocode 8: Design of structures for earthquake resistance, Part 1: General rules, seismic actions and rules for buildings", Committee for Standarization, Design. European Committee for Standardization, Brussels, Belgium.

CEN, 2004b. Comité Européen de Normalisation (2004a) "European Standard EN 1998-1:2004 Eurocode 8: Design of structures for earthquake resistance. Greek National Annex 1–24.

CEN, 2004c. Comité Européen de Normalisation (2004a) "European Standard EN 1998-1:2004 Eurocode 8: Design of structures for earthquake resistance. Part 1: General rules, seismic actions and rules for buildings." Brussels.

CEN, European Committee for Standardization (CEN), 2004. Eurocode 8: Design of structures for earthquake resistance—Part 1: General rules, seismic actions and rules for buildings (EN 1998-1: 2004). Eur. Comm. Norm. Brussels 1.

Coleman, J.L., Bolisetti, C., Whittaker, A.S., 2015. Time-domain soil-structure interaction analysis of nuclear facilities. Nucl. Eng. Des. 298, 264–270. doi:10.1016/j.nucengdes.2015.08.015

Cosenza, E., Di Sarno, L., Maddaloni, G., Magliulo, G., Petrone, C., Prota, A., 2014. Shake tablel tests for the seismic fragility evaluation of hospital rooms. Earthq. Eng. Struct. Dymamics. doi:10.1002/eqe

Costa, A.A.A., Arêde, A., Penna, A., 2013. Free rocking response of a regular stone masonry wall with equivalent block approach: experimental and analytical evaluation. Earthq. Eng. Struct. Dyn. doi:10.1002/eqe

Dassault Systèmes, 2014. Abaqus 6.14 / Analysis User's Guide.

Dimitrakopoulos, E.G., DeJong, M.J., 2012. Revisiting the rocking block: closed-form solutions and similarity laws. Proc. R. Soc. 468, 2294–2318. doi:10.1098/rspa.2012.0026

Ding, Z., Xia, Z., 2014. Research of Wave Incoherence Effect of a Nuclear Power Plant on a Soft Soil Site, in:

ASCE International Conference on Sustainable Development of Critical Infrastructure, Shanghai, China.
European Commission, 1996. Seismic re-evaluation of operating nuclear power plants in European countries. Comparative Study on national practices, Directorate-General Environment, Nuclear Safety and Civil Protection, Report EUR 16245. doi:10.1177/0193723509343615
Hu, H.T., Liang, J.I., 2000. Ultimate analysis of BWR Mark III reinforced concrete containment subjected to internal pressure. Nucl. Eng. Des. 195, 1–11. doi:10.1016/S0029-5493(99)00163-6
Hu, H.T., Lin, Y.H., 2006. Ultimate analysis of PWR prestressed concrete containment subjected to internal pressure. Int. J. Press. Vessel. Pip. 83, 161–167. doi:10.1016/j.ijpvp.2006.02.030
Huang, Y.-N., Whittaker, A.S., Luco, N., 2010. Seismic performance assessment of base-isolated safety-related nuclear structures. Earthq. Eng. Struct. Dyn. 39, 1421–1442. doi:10.1002/eqe.1038
Jeremić, B., Tafazzoli, N., Ancheta, T., Orbović, N., Blahoianu, A., 2013. Seismic behavior of NPP structures subjected to realistic 3D, inclined seismic motions, in variable layered soil/rock, on surface or embedded foundations. Nucl. Eng. Des. 265, 85–94. doi:10.1016/j.nucengdes.2013.07.003
Kabanda, J., Kwon, O.-S., Kwon, G., 2015. Time and frequency domain analyses of the Hualien Large-Scale Seismic Test. Nucl. Eng. Des. 295, 261–275. doi:10.1016/j.nucengdes.2015.10.011
Katsanos, E.I., Sextos, a. G., Elnashai, A.S., 2014. Prediction of inelastic response periods of buildings based on intensity measures and analytical model parameters. Eng. Struct. 71, 161–177. doi:10.1016/j.engstruct.2014.04.007
Kennedy, R.P., Short, S.A., Wesley, D.A., Lee, T.H., 1976. Effect on non-linear soil-structure interaction due to base slab uplift on the seismic response of a high-temperature gas-cooled reactor (HTGR), Nuclear Engineering and Design. Nucl. Eng. Des. 38, 323–355.
Konstantinidis, D., Makris, N., 2009. Experimental and analytical studies on the response of freestanding laboratory equipment to earthquake shaking. Earthq. Eng. Struct. Dyn. 38, 827–848. doi:10.1002/eqe
Kottke, A.R., Rathje, E.M., 2008. A semi-Automated procedure for selecting and scaling recorded earthquake motions for dynamic analysis. Earthq. Spectra 24, 911–932.
Kumar, S., Raychowdhury, P., Gundlapalli, P., 2015. Response analysis of a nuclear containment structure with nonlinear soil–structure interaction under bi-directional ground motion. Int. J. Adv. Struct. Eng. 7, 211–221. doi:10.1007/s40091-015-0092-7
Lysmer, J., Kuhlemeyer, R.L., Kulemeyer, R.L., 1969. Finite dynamic model for infinite media. J. Eng. Mech. Div. 95, 759–877.
Lysmer, J., Ostadan, F., Chin, C.C., 1999. Computer Program: SASSI2000 – A System for Analysis of Soil-structure Interaction. University of California, Berkeley, California.
Makris, N., Konstantinidis, D., 2002. The Rocking Spectrum and the Shortcomings of Design Guidelines.
Makris, N., Vassiliou, M.F., 2013. Planar rocking response and stability analysis of an array of free-□standing columns capped with a freely supported rigid beam. Earthq. Eng. Struct. Dyn. 42, 431–449. doi:10.1002/eqe
Muzumdar, A.J., Meneley, D.A., 2009. Large LOCA Margins in CANDU Reactors - an Overview of the COG Report, in: Proceedings of CNS 30th Annual Conference. May 31-June 3, Calgary, AB, pp. 1–17.
Nakamura, N., Akita, S., Suzuki, T., Koba, M., Nakamura, S., Nakano, T., 2010. Study of ultimate seismic response and fragility evaluation of nuclear power building using nonlinear three-dimensional finite element model. Nucl. Eng. Des. 240, 166–180.
Nakamura, N., S., I., Kurimoto, O., Miake, M., 2007. An estimation method for basemat uplift behavior of nuclear power plant. Nucl. Eng. Des. 237, 1275–1287.
Newmark, N.M., Hall, W.J., 1969. Seismic Design Criteria for Nuclear Reactor Facilities, in: 4th World Conference on Earthquake. Santiago, Chile.
Politopoulos, I., 2010. Response of seismically isolated structures to rocking-type excitations. Earthq. Eng. Struct. Dyn. 39, 325–342. doi:10.1002/eqe
Saxena, N., Paul, D.K., 2012. Effects of embedment including slip and separation on seismic SSI response of a nuclear reactor building. Nucl. Eng. Des. 247, 23–33. doi:10.1016/j.nucengdes.2012.02.010
Spears, R., Coleman, J., 2014. Nonlinear Time Domain Soil-structure Interaction Methodology Development. INL/EXT-14-33126. Idaho National Laboratory, Idaho Falls, Idaho. Taborda,.
Srinivasan, M.G., Kot, C.A., Hsieh, B.J., 1985. Comparison of Dynamic Characteristics of Fukushima Nuclear Power Plant Containment Building Determined From Tests and Earthquakes Office of Nuclear Regulatory Research Comparison of Dynamic Characteristics of Fukushima Nuclear Power Plant Containment Buil. Office of Nuclear Regulatory Research (NUREG), Argonne National Laboratory 9700 South Cass Avenue Argonne, IL 60439.
Voyagaki, E., Psycharis, I.N., Mylonakis, G.E., 2013. Rocking response and overturning criteria for free standing rigid blocks to single—lobe pulses. Soil Dyn. Earthq. Eng. 46, 85–95. doi:10.1016/j.soildyn.2012.11.010
Zhao, C., Chen, J., 2013. Numerical simulation and investigation of the base isolated NPPC building under

three-directional seismic loading 265, 484–496.